KCNJ2 mutation in short QT syndrome 3 results in atrial fibrillation and ventricular proarrhythmia

Makarand Deo[a], Yanfei Ruan[b], Sandeep V. Pandit[c], Kushal Shah[a], Omer Berenfeld[c], Andrew Blaufox[d], Marina Cerrone[b], Sami F. Noujaim[e], Marco Denegri[f], José Jalife[c,1,2], and Silvia G. Priori[b,f,g,2]

[a]Department of Engineering, Norfolk State University, Norfolk, VA 23504; [b]Cardiovascular Genetics Program, Leon Charney Division of Cardiology, New York University, New York, NY 10016 ; [c]Center for Arrhythmia Research, University of Michigan, Ann Arbor, MI 48109; and [d]Alexandra and Steven Cohen Children's Medical Center of New York, New Hyde Park, NY 11040; [e]Molecular Cardiology Research Institute, Tufts Medical Center, Boston, MA 02111; [f]Molecular Cardiology, Fondazione Salvatore Maugeri Istituto di Ricovero e Cura a Carattere Scientifico, 27100 Pavia, Italy; [g]Department of Molecular Medicine, University of Pavia, 27100 Pavia, Italy

Edited by Lily Yeh Jan, University of California, San Francisco, CA, and approved January 31, 2013 (received for review October 20, 2012)

We describe a mutation (E299V) in *KCNJ2*, the gene that encodes the strong inward rectifier K^+ channel protein (Kir2.1), in an 11-y-old boy. The unique short QT syndrome type-3 phenotype is associated with an extremely abbreviated QT interval (200 ms) on ECG and paroxysmal atrial fibrillation. Genetic screening identified an A896T substitution in a highly conserved region of *KCNJ2* that resulted in a de novo mutation E299V. Whole-cell patch-clamp experiments showed that E299V presents an abnormally large outward I_{K1} at potentials above −55 mV ($P < 0.001$ versus wild type) due to a lack of inward rectification. Coexpression of wild-type and mutant channels to mimic the heterozygous condition still resulted in a large outward current. Coimmunoprecipitation and kinetic analysis showed that E299V and wild-type isoforms may heteromerize and that their interaction impairs function. The homomeric assembly of E299V mutant proteins actually results in gain of function. Computer simulations of ventricular excitation and propagation using both the homozygous and heterozygous conditions at three different levels of integration (single cell, 2D, and 3D) accurately reproduced the electrocardiographic phenotype of the proband, including an exceedingly short QT interval with merging of the QRS and the T wave, absence of ST segment, and peaked T waves. Numerical experiments predict that, in addition to the short QT interval, absence of inward rectification in the E299V mutation should result in atrial fibrillation. In addition, as predicted by simulations using a geometrically accurate three-dimensional ventricular model that included the His–Purkinje network, a slight reduction in ventricular excitability via 20% reduction of the sodium current should increase vulnerability to life-threatening ventricular tachyarrhythmia.

cellular electrophysiology | computer models | genetics | ion channels | channelopathies

The short QT syndrome (SQTS) is an inherited arrhythmogenic disorder characterized by a remarkably abbreviated repolarization and a predisposition to supraventricular and ventricular arrhythmias in the absence of detectable structural heart disease (1). Mutations found in SQTS patients in the genes encoding potassium channels cause "gain of function," whereas mutations found in the alpha 1C subunit of the voltage-dependent L-type Ca^+ channel (*CACNA1C*), the beta 2b subunit of the voltage dependent Ca^{2+} channel (*CACNB2B*) and the alpha2/delta subunit 1 of the voltage dependent Ca^{2+} channel (*CACNA2D1*) cause "loss of function" (1, 2). In 2005, we reported a mutation (D172N) in the strong inward rectifier K^+ channel protein (Kir2.1), which is coded by *KCNJ2*, in an SQTS patient: Functional characterization revealed that D172N shows an increased outward component of the inward rectifier current I_{K1} (3). Computer simulation demonstrated that D172N leads to a shortening of the QT interval and predisposes the heart to develop reentrant arrhythmias. Here we report a different *KCNJ2* mutation (E299V) identified in a child with a remarkably short QT interval and atrial fibrillation (AF). In vitro expression shows that E299V severely impairs the inward rectification properties of the Kir2.1 channel, thus representing a unique mechanism for *KCNJ2*-related SQTS. Numerical experiments predict that absence of inward rectification should result in extreme shortening of action potential duration (APD) and an exceedingly short QT interval. In addition, simulations using a 3D ventricular model predict that slight changes in excitability greatly increase vulnerability to spontaneous bundle branch reentry and ventricular tachycardia (VT) as a result of exceedingly short Purkinje fiber APD. Further, the models suggest a mechanism for the vulnerability to recurrent paroxysmal AF in this patient.

Results

Cardiac Evaluation of the Proband. An 11-y-old boy was referred to our attention with a history of recurrent paroxysmal AF and mild left ventricular dysfunction. The patient had experienced his first episode of AF at the age of 8 y. An abnormally short QT interval was noticed on ECG, which showed a QRS merged with the T wave and absence of a distinctive ST segment in all leads (Fig. 1). Peaked T waves were present, particularly on the left precordial leads. Interestingly, ventricular arrhythmias had never been documented on Holter or during exercise stress test. A 12-lead Holter recording showed episodes of paroxysmal AF with an average ventricular response of 98 beats per minute (bpm) (minimum 54 bpm, maximum 172 bpm, Fig. 1*A*) and confirmed the presence of a short QT interval that failed to adapt to heart-rate changes (Fig. 1*B*). No ventricular arrhythmias were detected. Cardiac MRI showed normal volumes of the four chambers. Both left and right ventricles presented mild to moderate hypokinesis in all segments (left ventricular ejection fraction, 41%; right ventricular ejection fraction, 38%). There was no evidence of myocardial fibrosis, inflammation, or infiltration. After cardioversion the patient was placed on amiodarone and beta blockers to prevent AF recurrence. At a follow-up visit the patient was in sinus rhythm, the ejection fraction recovered, and the left ventricular hypokinesis disappeared, suggesting that both were most likely related to a cardiomyopathy caused by the rapid AF rate. The parents of the child had unremarkable ECGs and reported no family history of sudden cardiac death.

Genetic Analysis. DNA analysis was performed by FAMILION (PGxHealth, Transgenomics, Inc, Omaha, NE) and included screening of genes present in the SQTS screening panel. A single

Author contributions: J.J. and S.G.P. designed research; M. Deo, Y.R., S.V.P., K.S., A.B., and M. Denegri performed research; J.J. contributed new reagents/analytic tools; M. Deo, Y.R., S.V.P., K.S., O.B., M.C., S.F.N., J.J., and S.G.P. analyzed data; and M. Deo, J.J., and S.G.P. wrote the paper.

The authors declare no conflict of interest.

Freely available online through the PNAS open access option.

This article is a PNAS Direct Submission.

[1]To whom correspondence should be addressed. E-mail: jjalife@umich.edu.

[2]J.J. and S.G.P. contributed equally to this work.

This article contains supporting information online at www.pnas.org/lookup/suppl/doi:10.1073/pnas.1218154110/-/DCSupplemental.

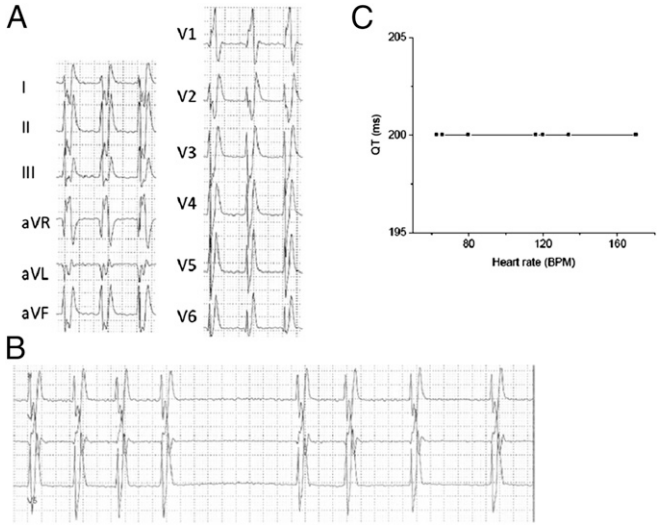

Fig. 1. (*A*) Twelve-lead ECG Holter recording showing atrial fibrillation (heart rate,120 bpm) with markedly shortened QT interval (QT 200 ms, paper speed 25 mm/s). (*B*) Twelve-lead ECG Holter recording showing atrial fibrillation (heart rate, 60 bpm) with short QT interval (QT 200 ms). (*C*) The flat relationship between heart rate and QT interval indicates lack of adaptation of QT interval to changes in cycle length.

base-pair substitution (A to T at nucleotide 896, A896T) was found in the *KCNJ2* gene, resulting in an amino acid change from glutamic acid to valine in the Kir2.1 channel (E299V). This residue is located within a highly conserved region of the Kir2.1 cytoplasmic terminal (Fig S1). The A896T substitution was not present in any of 400 control subjects. Parents were negative for the mutation *KCNJ2* A896T.

Cellular Localization of WT-Kir2.1/E299V-Kir2.1 and Assembly of Kir2.1 Tetramers. We verified the subcellular localization of the WT- and E299V-Kir2.1 proteins by Western blot analysis after transient transfection in human embryonic kidney cell line (HEK) 293 cells. Total lysates from WT and E299V were processed to obtain cytoplasmic and enriched plasma membrane fractions. Total lysates and single fractions were processed by immunoblot with anti-Kir2.1 antibody. As shown in Fig. 2*A*, the E299V-Kir2.1 mutant is expressed and both the level of expression and subcellular distribution overlap with WT.

Next, trafficking of the tagged E299V Kir2.1 protein was confirmed by immunofluorescence to highlight the plasma membrane distribution in transfected HEK 293 cells. The epitopes, Myc (polypeptide protein tag derived from the human proto-oncogene *c-myc*) and HA (hemagglutinin), were incorporated into an external site that did not interfere with channel properties (4). As shown in Fig. 2*B*, both Myc-E299V-Kir2.1 and HA-WT-Kir2.1 localize at the cell membrane, suggesting that the mutation does not cause a trafficking defect.

Immunoprecipitation studies were performed using differently tagged Kir2.1 subunits in HEK293 cells at a 1:1 ratio. Recovered immunoprecipitates on anti–Myc- or anti–HA-bound beads were resolved by SDS/PAGE, and the HA/Myc-tagged channel interaction was assessed using anti-HA or anti-Myc antibodies in immunoblots (Fig. 2*C*). The Myc-tagged subunits of WT-Kir2.1 and E299V-Kir2.1 were able to immunoprecipitate the corresponding HA-tagged subunits. These data demonstrated the ability of WT and E299V proteins to give rise to a homotetrameric Kir2.1 channel. In the presence of the cotransfected Myc-E299V-Kir2.1 and HA-WT-Kir2.1 constructs we demonstrated the coimmunoprecipitation of the WT and mutant subunits using two independent approaches (immunoprecipitation with anti-Myc and anti-HA, Fig. 2*C*), which confirmed that WT and mutant subunits were able to coassemble and form heterotetrameric Kir2.1 channels.

Cellular Electrophysiology. Functional characterization of the overexpressed WT and E299V in HEK293 cells demonstrated inward currents at potentials between −120 and −90 mV. However, the inward current generated by the E299V mutant channel was significantly reduced compared with WT (Fig. 3*A*); at −100 mV, inward current density was −58.2 ± 9.7 pA/pF in E299V ($n = 8$) vs. 138.7 ± 10.8 pA/pF in WT ($n = 11$; $P < 0.01$). At more positive voltages the WT channel showed inward rectification and inactivated completely near −30 mV (1.5 ± 0.3 pA/pF, at potential 0 mV). By contrast, the E299V channels showed a major impairment of the inward rectification property: At 0 mV, E299V Kir2.1 current was 56.5 ± 10.4 pA/pF ($P < 0.001$, vs. WT). Fig. 3*B* shows representative traces recorded from WT, E299V, and WT/E299V, elicited by voltage-clamp steps (duration 400 ms) from −100 mV to +40 mV, applied from a holding potential of −70 mV. In the current–voltage relationship shown in Fig. 3*A*, the voltage was adjusted to the liquid junction potential of 15 mV. As expected, cotransfection of the WT and mutant constructs gave intermediate values. The inward currents were 102.6 ± 7.8 pA/pF at −100 mV ($n = 6$). The inward rectification was slightly attenuated; at 0 mV, WT/E229V Kir2.1 current was 42.1 ± 6.1 pA/pF ($P < 0.001$, vs.

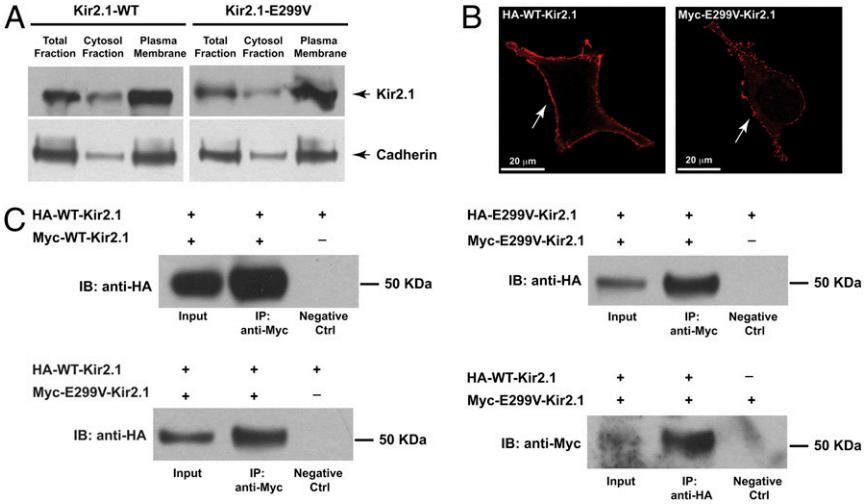

Fig. 2. (*A*) Subcellular distribution of WT- and E299V-Kir2.1 expression in HEK293 cells by immunoblot anti-Kir2.1. Antibody anti-cadherin was used as loading control. (*B*) Plasma membrane localization (white arrows) by immunofluorescence with anti-HA and anti-Myc antibody in nonpermeabilized HEK293 cells of HA-tagged WT channel (*Left*) and Myc-tagged E299V-Kir2.1 protein (*Right*). (Scale bar, 20 μm.) (*C*) Analysis of the protein–protein interaction by immunoprecipitation (IP) with HA-WT-Kir2.1, Myc-WT-Kir2.1, Myc-E299V-, and HA-E299V-Kir2.1 protein in HEK293 cells in different combinations as indicated. Data show that E299V-Kir2.1 localizes on plasmalemma membrane and is able to assemble in homo- and hetero-tetrameric Kir2.1 channels. IB, immunoblotting antibody.

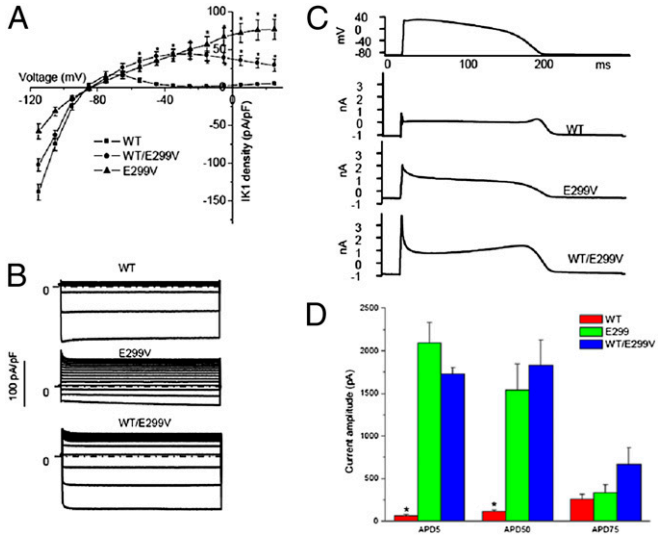

Fig. 3. (*A*) Current–voltage relationships. At each voltage from −55 to 25 mV, the current densities of E299V and WT/E299V are significantly larger than the WT ($P < 0.001$). (*B*) Representative currents for WT, E299V, and WT/E299V. Currents were elicited by 400-ms depolarizing voltage steps from −100 to +40 mV and from a holding potential of −70 mV. (*C*) Representative currents for WT, E299V, and WT/E299V elicited by action potential command signals as voltage protocol. (*D*) The current amplitudes at APD_5, APD_{50}, and APD_{75}, *$P <$ 0.01 vs. E299V and WT/E299V.

WT). There was no modification of reversal potentials (−86.4 ± 1.6, −85.9 ± 1.8, and −85.7 ± 2.3 for WT, E299V, and WT/E299V, respectively; not statistically significant). The ratio of the current amplitudes at +40 and −100 mV was calculated as an index of the rectification (Fig. S2). The indexes of WT, WT/E299V, and E299V were 0.03 ± 0.01, 0.49 ± 0.09, and 1.17 ± 0.11, respectively ($P < 0.01$, WT < WT/E299V < E299V, $n = 7$ for each group). Thus, the E299V mutation impairs rectification substantially but the heteromultimeric WT/E299V complex partially rescues rectification. These results confirm the previously demonstrated importance of the negative charge of E299 in the Kir2.1 sequence in controlling inward rectification (5). However, as illustrated in Fig. S2 *A* and *B*, the kinetics of activation were altered in such a way that E299V had significantly faster activation than WT, but the activation was significantly slower than WT at all voltages when WT and E299V were coexpressed. These data suggest that the E299V and WT isoforms may form heteromultimeric complexes and that their interaction somehow impairs function, whereas the homomeric assembly of E299V mutant proteins actually results in a gain of function.

Action potential clamp recordings in HEK293 cells demonstrated that WT Kir2.1 current rapidly decreased after membrane depolarization and exhibited a small repolarizing current during action potential plateau (Fig. 3*C*). At the end of repolarization, the WT Kir2.1 recording showed an increased outward repolarizing current consistent with the contribution of Kir2.1 to the terminal phase of repolarization. The E299V trace presented an early large outward current during the action potential voltage clamp, and the shape of the current was consistent with the loss of inward rectification of E299V. The WT/E229V Kir2.1 current gave an intermediate result. Current amplitudes for E299V and WT/E229V at APD_5 and APD_{50} were significantly larger than WT ($n = 6$–7 for each group), whereas current amplitudes at APD_{75} were comparable among three groups (Fig. 3*D*). Therefore, the severely impaired inward rectification in both heterozygous and homozygous conditions leads to a large outward current during the early phase of the action potential that dramatically shortens the APD.

Numerical Results. ***E299V shortens the action potential duration.*** To gain insight into the underlying electrophysiological phenotype and potential arrhythmogenic risk of the proband, we conducted computer simulations at various levels of integration using single-cell, 2D, and 3D models of cardiac excitation and propagation. Fig. 4*A* shows the simulated action potentials (APs) in human ventricular myocyte (VM) models (ORd) for WT/E299V, E299V, WT/D172N, and D172N compared with WT (see Fig. S3 for current-voltage relationships used in the simulations). Excessive outward component and absence of I_{K1} rectification resulted in significantly abbreviated APs (56% and 67% APD_{80} reduction in WT/E299V and E299V, respectively). However, simulation of the previously reported SQT3 mutation (WT/D172N and D172N) (3) showed an increase in the slope of phase-III repolarization without significant reduction in the APD. In Fig. 4*B*, significantly shortened APDs at all pacing frequencies and flat restitution curves (APD_{80}) for WT/E299V and E299V are evident. This lack of rate dependence is in line with the absence of QT interval variations with heart rate seen in the patient (Fig. 1).

E299V shortens the QT interval. Fig. S4 shows pseudo-ECGs obtained during propagation in a 2-cm-long cable (shown by the *Inset*) composed of endocardial and epicardial tissue. In this model we reproduced the important features of the ECGs obtained in both D172N and E299V mutations. For WT/D172N and D172D, the QT interval did not change significantly, but as previously demonstrated (3), the T wave was tall and asymmetrical. Conversely, for the mutation here described (WT/E299V and E299V), the QT interval was so short that the QRS merged with the T wave and the ECG trace presented no ST segment. Peaked T waves were also present in both simulated homozygous and heterozygous conditions. Thus, Fig. S4 shows fundamental differences in the clinical phenotype of E299V vs. D172N mutations.

E299V increases ventricular reentry vulnerability. In Fig. S5*A*, we systematically investigated the consequences of premature stimulation (S1–S2 protocol) and constructed "vulnerability-to-reentry" grids (Fig. S5*B*). The S1–S2 interval window that produced reentry (R) shifted toward shorter intervals in WT/E299V and E299V and was wider in E299V compared with WT and D172N. In addition, the excitability was significantly reduced in E299V owing to the very large I_{K1}, which resulted in rotor meandering and non-sustained reentry (8.79 Hz). As shown in Fig. S5*C*, WT/E299V, however, produced sustained reentry with a frequency (8 Hz) that

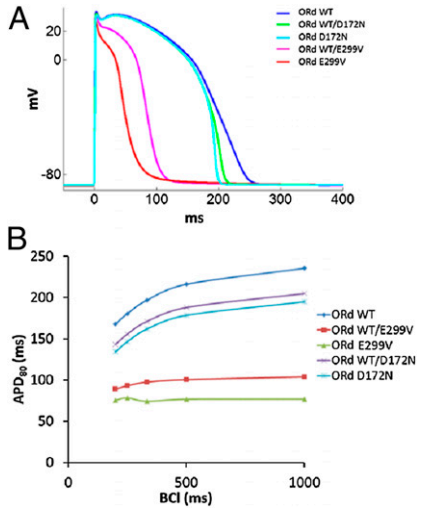

Fig. 4. (*A*) Simulated action potentials (APs) during 1-Hz pacing for SQT3 mutations using O'Hara et al. (20). Human VM model (ORd). (*B*) APD restitution properties for the mutations showing significant shortening of APDs at all basic cycle lengths (BCLs) and a flat restitution in WT/E299V and EV299.

was two times faster than WT (4 Hz). The R windows and frequencies of reentry in WT/D172N and D172N were similar to that in WT (4.66 and 4.95 Hz, respectively).

The simulated ECGs of the patient diagnosed with the E299V mutation exhibited a split QRS complex with an amplified T wave during sinus rhythm. To investigate the cause of such a peculiar ECG, we implemented the mutation in a 3D anatomical model of rabbit ventricles including a well-characterized Purkinje system (PS) (6, 7). Fig. S6 shows sequential snapshots of PS and ventricular excitation for each condition during a sinus beat. In the WT (Fig S6*A*), the sinus beat conducted via the His bundle and distal PS network excited both ventricles uniformly and synchronously; the entire cycle required 150–300 ms. In contrast, in the E299V condition (Fig S6*B*), left ventricular (LV) and the right ventricular (RV) excitation were not uniform (72–90 ms) and the excitation of the RV was appreciably delayed. The resulting ECGs exhibited striking similarities with the actual ECG of the proband showing wide and notched QRS morphology, as well as asymmetrical and tall T-wave merging with the QRS (Fig. 1).

E299V mutation is potentially proarrhythmic. The 3D simulations revealed that the significant APD reduction in the ventricular myocardium and the PS produced by the E299V mutation exposed the ventricles to the danger of arrhythmia initiation even with the slightest alteration in the conduction properties. Because of the extremely short APD, the PS was ready to be excited immediately after conducting the sinus beat to the ventricles and provided potential functional accessory pathways to allow the already nonuniform ventricular excitation to reenter retrogradely through the Purkinje branches. One such scenario is shown in the simulation presented in Fig. 5, where the excitability of the ventricles was slightly reduced by reducing the sodium current amplitude by 20% to mimic conditions of hyperkalemia (*Materials and Methods*). The pseudo-ECG presented in Fig. 5*B* shows the spontaneous initiation of arrhythmia at 2,600 ms. Immediately after the fourth sinus beat activation, an already excitable Purkinje branch in the septum of the LV (see a in Fig. 5*A*) was reactivated; it conducted the impulse retrogradely toward the right bundle branch (see b in Fig. 5*A*). This premature excitation depolarized the RV (see c in Fig. 5*A*); thereafter, the impulse was conducted transseptally back to the LV (see d in Fig. 5*A*) and was again picked up by the Purkinje branch at the LV septal wall. Thus, bundle branch reentry was initiated, which resulted in sustained VT (Fig. 5*C*).

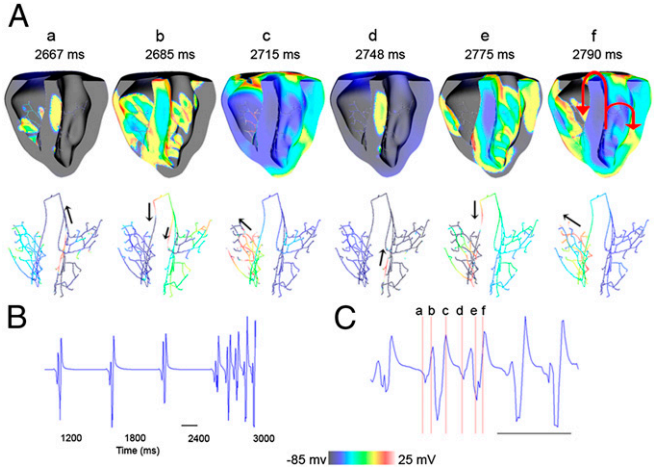

Fig. 5. Bundle branch reentry at reduced excitability (80% I_{Na}) in E299V. (*A*) Sequential snapshots of excitations during reentry in cross-sectional view of the ventricles (*Upper*) and the conduction through the PS (*Lower*). (*B*) Simulated ECG during reentry. (*C*) Enlarged region corresponding to the snapshots in *A*.

Subpanel f in Fig. 5*A* shows two reentry pathways observed in this case. The main reentry circuit included the left and right bundle branches and transseptal conduction. The other passive circuit was observed within the LV fascicles. The conditions for reentry were established as a result of significant APD abbreviation within the PS, which reversed the APD gradient that normally exists in the human heart between the PS and the ventricular myocardium and that serves as a natural protection against reexcitation. In the E299V condition, the extremely abbreviated APDs of the PS renders it available for retrograde conduction almost immediately after a previous excitation, thus making the heart vulnerable to develop arrhythmias. We observed several arrhythmia initiation patterns when either the tissue conductivity or excitability was slightly altered.

Predicting the mechanism of paroxysmal AF. The E299V proband exhibited multiple recurrent episodes of paroxysmal AF. Therefore, in an effort to understand the underlying mechanism, we studied the effects of the E299V mutation using the recently published Grandi-Pandit (GP) model of the human atrial cell (8). I_{K1} formulations in the human atrial cell (GP) model were fitted to match the experimental current–voltage relationships in WT, WT/E299V, and E299V (Fig. S3*A*). As illustrated in Fig. 6*A*, the morphology and duration of the simulated atrial action potentials of WT/E299V and E299V were similar and were significantly abbreviated compared with WT (48% reduction in APD_{80}). In Fig. 6*B*, similar to the VM model, the restitution curves for the atrial cells in WT/E299V and E299V were flat compared with WT. We also constructed vulnerability grids for the atrial model similar to the VM model (Fig. S5) using an S1–S2 crossfield stimulation protocol as shown in Fig. 6*C*. For the WT model, we could not produce reentry for any S1–S2 interval. However, reentry windows were observed for both WT/E299V and E299V. The reentry window in E299V was wider than that in WT/E299V.

Discussion

We report a de novo *KCNJ2* mutation, E299V, in a SQTS patient with a markedly abbreviated QT interval and atrial fibrillation (Fig. 1). Functional characterization of the Kir2.1 E299V mutation performed in HEK cells demonstrated that the mutant E229V subunits are able to assemble as homo- and heterotetrameric Kir2.1 channels (Fig. 2). Patch-clamp studies demonstrated a severely impaired inward rectification, resulting in a gain of function of the I_{K1} current that is likely to be responsible for shortening of the QT interval. As predicted also by our computer simulations, the extreme shortening of the QT interval is likely to be associated with substantial APD abbreviation brought about by the substantial increase in the outward component of I_{K1}. In addition, the simulations predict that the mutation increases vulnerability to reentrant arrhythmias, particularly under conditions that would decrease sodium channel availability. Finally, in conformation with the patient's electrical phenotypes, the simulations also predict an increased vulnerability to atrial fibrillation. However, as implied also by the simulation results, sodium channel blockers should not be used in this patient to control atrial fibrillation.

E299V Mutation Abolishes Inward Rectification. Previous studies have demonstrated that inward rectification in Kir channels is the result of voltage-dependent blockade by intracellular Mg^{2+} and/or polyamines (9). The rectification is regulated by two different negatively charged sites, one in the transmembrane domain, involving D172, and the other in the cytoplasmic region, involving E224, E299, D255, and D259 (5). The glutamic acid at position 299 is highly conserved in Kir2.1 channels in different species (Fig. S1). It is located at the cytoplasmic domain of Kir2.1 channels and together with other negatively charged residues forms the inner vestibule of the channel pore, which determines the strength of inward rectification of I_{K1} (10). It has been demonstrated that the substitution of glutamic acid at position 299 with a neutral amino

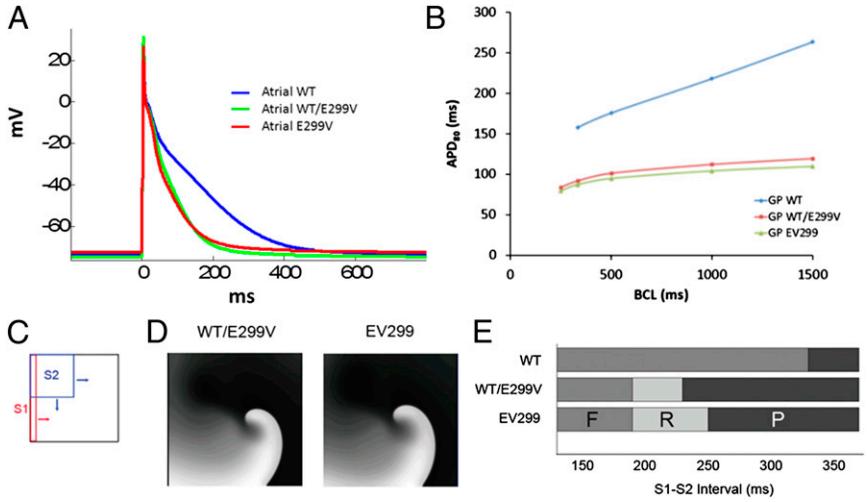

Fig. 6. (*A*) Simulated APs in human atrial cell model (GP model, ref. 8) during 1-Hz pacing in control (WT), WT/E299V, and EV299. (*B*) APD restitution properties for the models showing significant shortening of APDs at all basic cycle lengths (BCLs) and a flat restitution in WT/E299V and E299V. (*C*) Cross-field S1–S2 stimulation protocol used to assess arrhythmogenicity in human atrial cell model (GP). (*D*) Snapshots of a spiral wave reentry obtained in control (WT), WT/E299V, and E299V. (*E*) Vulnerability to reentry grid constructed by summarizing the outcome at varying S1–S2 intervals. F, failure to conduct S2 stimulus; P, normal propagation of S2 beat; R, reentry.

acid such as serine leads to weak inward rectification properties of Kir2.1 (11). It also decreases the sensitivity of the channel to the block by polyamine or Mg^{2+}. Given the neutral amino acid (E to V) at position 299, we anticipated a disruptive effect of the mutation on the rectification properties. As expected, E299V mutation almost completely lacks inward rectification. Very recently, Hattori et al. (12) described an interesting *KCNJ2* mutation (M301K) in an 8-y-old girl who had an extremely abbreviated QT interval (QTc = 194 ms) and paroxysmal AF (12). When M301K mutant channels (homozygous condition) were expressed alone, they were entirely nonfunctional, whereas when cells were cotransfected with both equimolar WT and M301K (heterozygous condition), their potassium currents rectified very weakly. These data are at variance with what we observed in the E299V mutant channels: Expression in HEK293 cells of the E299V mutant (homozygous condition) shows Kir2.1 current with negligible rectification, which complements the Western blot data (Fig. 2*A*) demonstrating that homomeric E229V channels are able to traffic to the cell membrane. Hattori et al. (12) showed that the coexpression of M301K with WT leads to increased trafficking of channels but they do not provide evidence that the mutant protein is able to form heterotetrameric channels, whereas we have demonstrated that E299V is able to interact with WT (Fig. 2*C*). Altogether, the trafficking and assembling properties of the E299V and M301K mutations seem to be significantly different from each other despite their close proximity within the C terminal of the Kir2.1 channel and their similar effects on I_{K1} rectification.

Based on 2D NMR spectroscopy, isothermal calorimetry, and mutagenesis studies conducted by Osawa et al. (9) for an analogous mutation (E300N) in Kir3.1, we hypothesize that in the case of the E299V, substitution of a negatively charged residue (glutamic acid) with a hydrophobic residue (valine) significantly disrupted spermine binding to its receptor in the intracellular pore of Kir2.1, possibly by producing conformational changes in the Kir2.1 subunits, therefore impairing I_{K1} rectification. Heteromerization also likely contributed to the phenotype, in a manner that was different from that in the M301K case.

E299V Mutation Results in a Different Kind of SQT3. Cotransfection of the WT and E299V plasmids mimicking the heterozygous substrate of the patients yielded an intermediate situation between WT and/or E299V. The electrophysiological consequences of E299V are profoundly different from those of the D172N mutation that we reported as a unique *KCNJ2* mutation linked to SQTS (3), as well as the V93I mutation reported by Xia et al. (13) for a Chinese family with familial AF. Both D172N and V93I increase the outward current between −70 mV and −50 mV, thus causing sudden acceleration of the final phase of action potential repolarization that is responsible for an asymmetrically shaped T wave with a rapidly descending limb observed among mutation carriers. D172N, however, did not modify the rectification properties of the channel (3). This is in line with heterologous cell experiments in which the D172N mutation weakened inward rectification only slightly. In contrast, similar to the heterozygous M301K mutation (12), the E299V mutation had a more remarkable effect weakening rectification (Fig. 2; and figure 2 in ref. 12) and shortening QT (Fig. 1).

In our computer simulations, we have also compared the effects of E299V and D172N in a mathematical model of the human ventricular cells (Fig. 4). The similarities include the sharp final repolarization phase at the cellular level and T wave in both D172N and E299V mutations. However, in contrast with D172N, E299V shortens the action potential duration more substantially, on account of its markedly weak rectification. This leads to the absence of an ST segment in the ECG in the E299V patient (Fig. 1 and Fig. S4). Another important difference is the flattening of the APD restitution curve in the E299V mutations, compared with the downward shift in D172N; the former enables us to explain the lack of further QT abbreviation in the E299V patient at higher heart rates. The 3D computer simulations demonstrate that the loss of rectification also has implications for propagation of the cardiac impulse, and the resulting delayed activation causes the peculiar QRS alterations seen in the E299V patient (Fig. S6). Moreover, our simulations investigating the vulnerability window in a 2D sheet of ventricular cells suggest that although the S1–S2 interval for initiating reentry is very different, the width of actual window of vulnerability is not appreciably different between WT and either of the different SQT3 mutations (Fig. S5).

E299V Mutation Is Associated with AF but Not with VT/VF. The simulations also predict that E299V increases the vulnerability of the atria to reentry, which correlates well with the fact that the proband has experienced various episodes of paroxysmal AF. However, to this date, the patient has not presented with ventricular tachycardia/ventricular fibrillation (VT/VF). Similar to the V93I mutation reported by Xia et al. (13), the reason for the lack of ventricular arrhythmias remains unknown at this point. Nevertheless, as predicted by the 3D simulations (Fig. 5), any small change in excitability, for example by the use of class-I antiarrhythmic drugs to treat AF, should result in ventricular arrhythmias secondary to bundle branch reentry. Therefore, we can only speculate as to why no ventricular arrhythmias have developed in the E299V patient. We surmise that the highly predictable spatiotemporal organization of the specialized conducting system of the ventricles provides a high degree of protection against ventricular

arrhythmias in this patient. Such a high degree of organization and synchrony, which need not exist in the atria, would act to prevent or at least reduce the likelihood of reentry in the ventricles. Moreover, in this patient, the large amount of outward I_{K1} would prevent the formation of ectopic automaticity anywhere in the ventricles. However, a small decrease in I_{Na} density might be sufficient to tilt the balance toward increased ventricular vulnerability and result in polymorphic VF secondary to bundle branch reentry (Fig. 5).

Potential Therapeutic Approaches. Currently, the AF in this patient is being controlled effectively with amiodarone; to our knowledge, the patient has not experienced any ventricular arrhythmias. Nevertheless, as predicted by the simulations, caution should be exerted in this patient when attempting to treat his AF episodes with any agent leading to peak I_{Na} reduction, for example a class-I antiarrhythmic agent. Thus, in an attempt to predict which therapy might benefit this young patient in the event he develops ventricular arrhythmias, we first considered the possibility that a hypothetical drug capable of increasing the late sodium current might plausibly counteract the large outward current provided by the weakly rectifying E299V mutation. However, as demonstrated in Fig. S7 (Tables S1–S4 quantify the data), increasing I_{NaL} up to 100% produces no change in the voltage-dependent intracellular calcium transient or APD_{80}. Clearly, the exceedingly large outward I_{K1} overpowers any amount of inward depolarizing current coming through the late sodium current during the plateau. Interestingly, however, as shown in Fig. S8, increasing the L-type calcium current (I_{CaL}) 100% in the presence of the E299V mutation restored the originally reduced calcium transient above control levels, increased the action potential plateau, and slightly restored the APD toward control. Increasing I_{CaL} by 300 and 500% further prolonged the APD to some extent but produced huge, unphysiological increases in the intracellular calcium transient. From these data, one could predict a relatively mild antiarrhythmic effect if using a hypothetical I_{CaL} activator of the BayK 8644 type.

Obviously, the best way to restore the action potential duration toward control levels in this patient would be to promote inward rectification of the Kir2.1 channel. However, to our knowledge, no specific blocker of Kir2.1 exists that may have therapeutic potential. Tamoxifen (14) and chloroquine (15, 16) block Kir2.1 channels at low micromolar concentration but display prominent effects on other potassium, calcium, and sodium channels. Nevertheless, chloroquine has been shown to effectively terminate both atrial and ventricular fibrillation (16) and has been deemed to be more effective than flecainide as an antifibrillatory agent in a sheep model of stretch-induced atrial fibrillation (16, 17). However, its effects seem to be mediated in part by I_{Na} blockade, which makes chloroquine an unlikely therapeutic option for our patient with the E299V mutation. Other agents such as gamboric acid (18) and the antiprotozoal pentamidine (19) potently block Kir2.1 channels following chronic exposure but are less efficacious acutely. Future studies should be aimed at developing next-generation small molecules that could serve as patient-specific antiarrhythmic agents.

Materials and Methods

Experimental and numerical methods are presented in detail in *SI Materials and Methods*.

Site-Directed Mutagenesis. The *Kir 2.1-E299V* mutation was engineered into WT cDNA cloned in pcDNA3.1. Site-directed mutagenesis was carried out using a PCR-based strategy.

Transfection in HEK293 Cells. HEK 293 cells were transfected with 1.6 μg of plasmid DNA of Kir2.1-WT or Kir2.1-E299V mutant.

SDS/PAGE and Western Blotting. The expression analysis of WT-KCNJ2 and E299V-KCNJ2 was performed by Western blot.

ImmunoFluorescence. Immunofluorescence microscopy was used to detect the presence of Kir2.1 protein at the plasma membrane of HEK293-A cells.

Immunoprecipitation. The protein–protein interaction was studied with coimmunoprecipitation with Kir2.1 subunits tagged with different epitopes.

Cellular Electrophysiology. Functional characterization of WT and mutant channels was performed by patch clamp. Current recordings were performed at room temperature.

Numerical Methods. Model equations are presented in detail in *SI Materials and Methods, Numerical Methods*.

Human ventricular myocyte. A modified version of human VM model of O'Hara et al. (20) was used to simulate the cardiac action potential. The modified model is referred to as ORd.

Human atrial cell. The arrhythmogenic effects of WT/E299V and E299V mutations were also studied in human atria by conducting simulations using the Grandi-Pandit (GP) model (8).

ACKNOWLEDGMENTS. We thank Patrizia Vaghi and Centro Grandi Strumenti of the University of Pavia for technical assistance with the confocal microscopy facility. This work was supported by National Heart, Lung, and Blood Institute Grants P01-HL039707 and P01-HL87226 (to J.J.) and R00HL105574 (to S.F.N.), and grants from the Leducq Foundation (to J.J. and S.G.P.), Fondazione Veronesi "Modelli cellulari e terapia sperimentale dei difetti cardiaci associati a patologie aritmogene ereditarie" (to S.G.P.), Cassa di Risparmio delle Provincie Lombarde Grant pr.2008.2275 (to S.G.P.), and Ministry of Education, Universities Research Grant GR2009-1606636 (to S.G.P.).

1. Patel C, Yan GX, Antzelevitch C (2010) Short QT syndrome: From bench to bedside. *Circ Arrhythm Electrophysiol* 3(4):401–408.
2. Templin C, et al. (2011) Identification of a novel loss-of-function calcium channel gene mutation in short QT syndrome (SQTS6). *Eur Heart J* 32(9):1077–1088.
3. Priori SG, et al. (2005) A novel form of short QT syndrome (SQT3) is caused by a mutation in the KCNJ2 gene. *Circ Res* 96(7):800–807.
4. Ma D, et al. (2001) Role of ER export signals in controlling surface potassium channel numbers. *Science* 291(5502):316–319.
5. Pegan S, et al. (2005) Cytoplasmic domain structures of Kir2.1 and Kir3.1 show sites for modulating gating and rectification. *Nat Neurosci* 8(3):279–287.
6. Boyle PM, Deo M, Plank G, Vigmond EJ (2010) Purkinje-mediated effects in the response of quiescent ventricles to defibrillation shocks. *Ann Biomed Eng* 38(2): 456–468.
7. Deo M, Boyle PM, Kim AM, Vigmond EJ (2010) Arrhythmogenesis by single ectopic beats originating in the Purkinje system. *Am J Physiol Heart Circ Physiol* 299(4): H1002–H1011.
8. Grandi E, et al. (2011) Human atrial action potential and Ca2+ model: Sinus rhythm and chronic atrial fibrillation. *Circ Res* 109(9):1055–1066.
9. Osawa M, et al. (2009) Evidence for the direct interaction of spermine with the inwardly rectifying potassium channel. *J Biol Chem* 284(38):26117–26126.
10. Bichet D, Haass FA, Jan LY (2003) Merging functional studies with structures of inward-rectifier K(+) channels. *Natl Rev* 4(12):957–967.
11. Kubo Y, Murata Y (2001) Control of rectification and permeation by two distinct sites after the second transmembrane region in Kir2.1 K+ channel. *J Physiol* 531(Pt 3): 645–660.
12. Hattori T, et al. (2012) A novel gain-of-function KCNJ2 mutation associated with short-QT syndrome impairs inward rectification of Kir2.1 currents. *Cardiovasc Res* 93(4):666–673.
13. Xia M, et al. (2005) A Kir2.1 gain-of-function mutation underlies familial atrial fibrillation. *Biochem Biophys Res Commun* 332(4):1012–1019.
14. Ponce-Balbuena D, et al. (2009) Tamoxifen inhibits inward rectifier K+ 2.x family of inward rectifier channels by interfering with phosphatidylinositol 4,5-bisphosphate-channel interactions. *J Pharmacol Exp Ther* 331(2):563–573.
15. Rodríguez-Menchaca AA, et al. (2008) The molecular basis of chloroquine block of the inward rectifier Kir2.1 channel. *Proc Natl Acad Sci USA* 105(4):1364–1368.
16. Noujaim SF, et al. (2011) Structural bases for the different anti-fibrillatory effects of chloroquine and quinidine. *Cardiovasc Res* 89(4):862–869.
17. Filgueiras-Rama D, et al. (2012) Chloroquine terminates stretch-induced atrial fibrillation more effectively than flecainide in the sheep heart. *Circ Arrhythm Electrophysiol* 5(3):561–570.
18. Zaks-Makhina E, Li H, Grishin A, Salvador-Recatala V, Levitan ES (2009) Specific and slow inhibition of the kir2.1 K+ channel by gambogic acid. *J Biol Chem* 284(23): 15432–15438.
19. de Boer TP, et al. (2010) The anti-protozoal drug pentamidine blocks KIR2.x-mediated inward rectifier current by entering the cytoplasmic pore region of the channel. *Br J Pharmacol* 159(7):1532–1541.
20. O'Hara T, Virág L, Varró A, Rudy Y (2011) Simulation of the undiseased human cardiac ventricular action potential: Model formulation and experimental validation. *PLOS Comput Biol* 7(5):e1002061.